

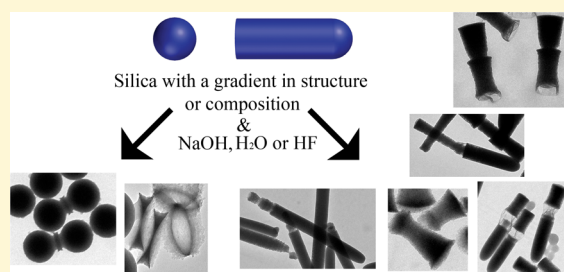
Sculpting Silica Colloids by Etching Particles with Nonuniform Compositions

Fabian Hagemans,^{*†} Wessel Vlug, Chiara Raffaelli, Alfons van Blaaderen,^{*} and Arnout Imhof^{*†}

Soft Condensed Matter, Debye Institute for NanoMaterials Science, Utrecht University, Princetonplein 1, 3584 CC, Utrecht, The Netherlands

Supporting Information

ABSTRACT: We present the synthesis of new shapes of colloidal silica particles by manipulating their chemical composition and subsequent etching. Segments of silica rods, prepared by the ammonia catalyzed hydrolysis and condensation of tetraethylorthosilicate (TEOS) from polyvinylpyrrolidone loaded water droplets, were grown under different conditions. Upon decreasing temperature, delaying ethanol addition, or increasing monomer concentration, the rate of dissolution of the silica segment subsequently formed decreased. A watery solution of NaOH (~mM) selectively etched these segments. Further tuning the conditions resulted in rod–cone or cone–cone shapes. Deliberately modulating the composition along the particle's length by delayed addition of (3-aminopropyl)-triethoxysilane (APTES) also allowed us to change the composition stepwise. The faster etching of this coupling agent in neutral conditions or HF afforded an even larger variety of particle morphologies while in addition changing the chemical functionality. A comparable step in composition was applied to silica spheres. Biamine functional groups used in a similar way as APTES caused a charge inversion during the growth, causing dumbbells and higher order aggregates to form. These particles etched more slowly at the neck, resulting in a biconcave silica ring sandwiched between two silica spheres, which could be separated by specifically etching the functionalized layer using HF.



INTRODUCTION

Instead of selectively adding material to build up a nanoparticle, it is also possible to selectively remove material of already formed particles to change their size and/or shape. Due to their high potential in chemical, electrical, and optical applications,^{1–3} a large variety of anisotropic particles have been developed following this principle. A common method used to create more complicated shapes is by making use of a template that can be sacrificed. Typically, colloidal templates are coated with a layer consisting of a different material than the template, so that the latter can be removed by chemical dissolution. Examples of anisotropic particles created this way are hollow spindles, cubes, ellipsoids, and peanuts but also particles with protrusions and cavities.^{4,5} Instead of using chemical dissolution, one can also make use of calcination. Here, a sacrificial layer is used consisting of a material that is eliminated a heat treatment. In such a way Nagao et al. were able to remove a polymer layer from between a silica core and a silica shell, in order to prepare hollow asymmetrical silica dumbbells.⁶

Instead of making use of the unequal solubility and/or rate of dissolution of two different materials, one can also make use of the different dissolution rates of certain sites on a nanoparticles consisting of only one material. Differences in chemical composition and structure within one particle result in different etching rates within the same particle. The local rate of dissolution of colloidal particles depends on the exact local composition and structure and is the product of a

thermodynamic driving force as given by the solubility but also a kinetic factor that depends on accessibility and diffusion rates. Many nanocrystals show distinct anisotropic dynamics in their dissolution in low concentration of acid: reactive and highly accessible sites at the ends are etched first, resulting in the deformation of these nanocrystals, of which many examples are given in a recent review.⁷ In the presence of silver ions, etching of gold nanorods mostly takes place at the sides of the gold rod resulting in dumbbell shaped particles.⁸ By first embedding these gold nanorods in a mesoporous silica shell, one can change the size of the rod inside the silica matrix by oxidative etching. Subsequent overgrowth with a different metal resulted in new material properties.⁹

The extent of the condensation reaction in the formation of silica particles, also known as the degree of condensation, also influences the local rate of dissolution. Silica with a low degree of condensation dissolves faster than silica with a high degree of condensation, simply because fewer siloxane bonds need to be broken.^{10,11} Differences in the degree of condensation between different synthesis methods were found for Stöber silica and silica particles grown in a microemulsion. For microemulsion particles 55% of the silicon atoms were found to be fully condensed as compared to >60% for Stöber silica.¹² Some

Received: February 17, 2017

Revised: March 17, 2017

Published: March 17, 2017

parameters that influence the condensation rate and degree of silica are the pH and the temperature.^{11,13} Besides a change in reaction conditions during growth, one can also apply a composition step during the growth of silica. Organo-silica co-condensed from tetraalkoxysilanes and alkyltrialkoxysilanes was found to dissolve faster in HF solutions than silica prepared from tetraalkoxysilanes alone¹⁴ as the degree of condensation will be lower than 4.^{15,16}

Differences in resistance to etching or differences in the rate of dissolution of the silica network have been used for the preparation of various types of particles. A well-known example is the rattler type particle: a silica shell that encapsulates a movable core. One way of preparing these particles is by exploiting the differences in structure and composition of the silica network.¹⁷ The silica grown latest in the synthesis was found to be more resistant against etching than silica grown at the start. This difference in the structure of the silica network was used to selectively etch the inner layer around a central gold core, while the outer layer was etched at a significantly lower rate and remained until the end. The outer layer of silica was found to be hardened by the reagents present in the preparative solution. Growing multiple shells around the particles resulted in a layered chemical structure, where upon etching each layer dissolved except for the silica at the boundaries between layers. It was found that this difference in dissolution rate became smaller upon incubating the particles in the preparative solution at 60 °C.¹⁷ In addition, it was found that even the solution in which Stöber silica is washed or stored after synthesis can have significant effect on dissolution rates of the particles.^{18,19}

Differences in the chemical composition can also be used to prepare anisotropic particles by etching. The etching rate of an organo-silica layer is different from that of a pure silica layer. The etching rate is increased due to the lower number of siloxane bonds of a silane coupling agent. As already mentioned, this principle was used to create rattler type particles. These particles consist of a pure silica core, an organo-silica layer, and a pure silica shell. Upon etching these particles in aqueous hydrofluoric acid (HF), the organo-silica layer etched significantly faster and could be removed through the outer silica layer which became only slightly more porous.¹⁴ The selectivity of differences in dissolution rates for different types of etchants can also be exploited to modify the particle shape further: double-shelled silica spheres were prepared by alternately using the base Na₂CO₃ and HF etching.²⁰

Instead of changing the chemical composition or structure, another way to change the dissolution rates is to protect the surface layer from etching. The polymer polyvinylpyrrolidone (PVP) was found to protect the surface and prevent etching whereas the inner parts dissolved much more easily.^{21,22} Instead of using a polymer, one can also prevent access to part of the silica interface of particles more drastically. Adsorbing modified silica spheres at a wax–water interface of a Pickering emulsion resulted in the etching of the hemisphere in contact with the aqueous phase. The part of the particles embedded in the wax was protected and remained unetched.²³

Recently, a new colloidal system consisting of silica rods was introduced.^{24,25} These rods grow from water rich emulsion droplets dispersed in a water poor continuous oil phase. The silica precursor requires water for the hydrolysis and subsequent condensation reaction. Therefore, growth mainly takes place from inside the water rich droplet and not from the water poor oil phase. This anisotropic supply of the precursor

results unidirectional growth of a rodlike particle. The particles consist of a rounded end and a flat end; the silica at the flat end is grown last. Due to slow growth of silica from the oil phase as well, a thin shell is also grown on that part of the rod that is in contact with the oil. Because of the longer exposure to the growth solution of the tip and the shorter exposure of the end, this outer shell decreases in thickness along the length of the rod. The particles are monodisperse enough that they readily form smectic liquid crystal phases. They can be easily functionalized during or after synthesis. Incorporation of a dye coupled to 3-aminopropyltriethoxysilane (APTES) from the start of the reaction results in a fluorescent gradient pattern.²⁶ Close inspection of this fluorescence pattern has shown that the dye is mainly located in an outer thin silica shell.²⁷ However, upon incorporating APTES alone, followed by the fluorescent labeling with FITC (fluorescein isothiocyanate) afterward, a homogeneous distribution of fluorophores was found. This pattern of fluorescence indicates that the local chemical composition of the particle can be tuned by changing the properties of the reacting species.

Recent advances in the synthesis of silica rods, using the above-mentioned emulsion based procedure, have resulted in a variety of experimental methods to change the shape of the particles during their growth. Two important parameters that influence the growth of these particles are temperature and ethanol concentration. Upon increasing the temperature or the ethanol concentration, the diameter of the rod decreases from that point onward in the reaction, which is thought to be the result of a decrease in the water droplet size.^{28,29} The concentration of base has also been found to influence the locus of growth; an increased growth at the interface results in the growth of hollow rods.³⁰ Even without changing any of these conditions externally, it is expected that the reaction conditions change in time anyway as during particle growth water and silicon alkoxide are consumed and ethanol is produced. These changes in the reaction conditions lead to a subtle gradient in degree of condensation along the rod's length. This gradient was previously used for the transformation of rods into cone shaped particles, while, depending on the reaction conditions, biconcave rods could also be synthesized.²⁷

Here, we significantly expand on the possibilities of sculpting silica colloids by changing the reaction temperature, precursor concentration, and ethanol concentration. Temperature, reagent concentration, and ethanol concentration were found to influence the local chemical structure. We show that these gradients in composition and structure can be used to change the shape of the particles by etching the particles in low concentrations of etchant (using NaOH, HF, or even pure water solutions). These methods were also combined in one synthesis to form more complicated gradients and, through these, an even larger variety of new shapes in silica particles. The chemical composition of silica rods could be modified by the incorporation of APTES, and the segment grown was found to dissolve faster in water than regular silica. In this paper, we not only demonstrate sculpting of rod-like silica particles but also illustrate with spherical silica particles that the methodology can be generally applied to all kinds of silica structures. For instance, under certain etching conditions dumbbell shaped core–shell particles, formed by aggregation during the growth of layers around silica spheres, were found to etch from the outside specifically. The middle segment where the spheres met dissolved more slowly than the rest of the spheres. The

resulting biconcave segment could be easily detached by subsequently etching the particles in HF.

RESULTS AND DISCUSSION

Rodlike silica particles with steps in degree of siloxane cross-linking were synthesized by varying the temperature, ethanol concentration, and TEOS concentration at different stages of the rod growth (see [Experimental Section](#)). This reaction protocol resulted in silica rods with segments of different compositions along the length of the rod. These different segments along the length of the silica rods therefore also had a different sensitivity to the etchant NaOH. Exposure to the etching solution thus produced sculpted colloids.

We initially investigated the effect of varying the temperature, ethanol concentration, and TEOS concentration on the resulting shape of the silica rod. Thereafter, we explored how the shapes were further changed by etching of these particles.

We found that not only the degree of local silica condensation but also the accessibility of sections of the particles to the etchant are of great importance to the resulting silica rod morphology. A balance between the rate of dissolution as determined by the degree of siloxane bonds formed or the degree of condensation and the accessibility of the base in a colloidal silica particle was then used to obtain a new shape by a simple two step etching protocol.

Effect of Modifying Temperature at Various Times during the Silica Rod Growth on the Resulting Morphology. It is known that decreasing the temperature during the growth of silica rods results in an increase of the diameter of the rod, and an increase in reaction temperature results in a decreased diameter. These effects are explained by a change of the water droplet size in accordance with the diameter change of the rods. By designing a procedure with multiple growth steps at various temperatures, segmented rods can be prepared, as has been previously shown by Datskos et al.²⁸

First, we prepared silica rods, consisting of a segment grown at 50 °C followed by a segment grown at 5 °C ([Figure 1a](#) and scheme in [Figure 1](#)). This resulted in rods with two segments. Etching these silica rods, with 1 mM NaOH, resulted in particles in which the second segment is etched so much faster that it ends up being etched almost completely even though it was initially thicker, whereas the first segment seems to have remained untouched ([Figure 1b](#)). We hypothesize that this selective etching occurs because of the varying microstructure of the silica network in the segments. This varying microstructure arises from growing the silica rod segments at varying temperatures, which influences the degree of condensation of silica. A lower temperature resulted in a decreased degree of condensation with a faster dissolution rate, whereas an increased temperature resulted in an increased degree of condensation and thus a network that dissolves more slowly.^{11,12,31}

Looking more closely at the etched segment in the particles in [Figure 1b](#), we see that it shows “growth rings”. We hypothesize that these “growth rings” arise from of the inhomogeneous cooling of the sample during the silica rod growth. Thus, various growth conditions actually exist in the solution as a result of the rapid cooling down process. Furthermore, the slow gradient in composition, which was initially observed for silica rods grown at room temperature,²⁷ cannot be observed in these particles; the first segment of the rod does not transform into a concave shape upon etching with

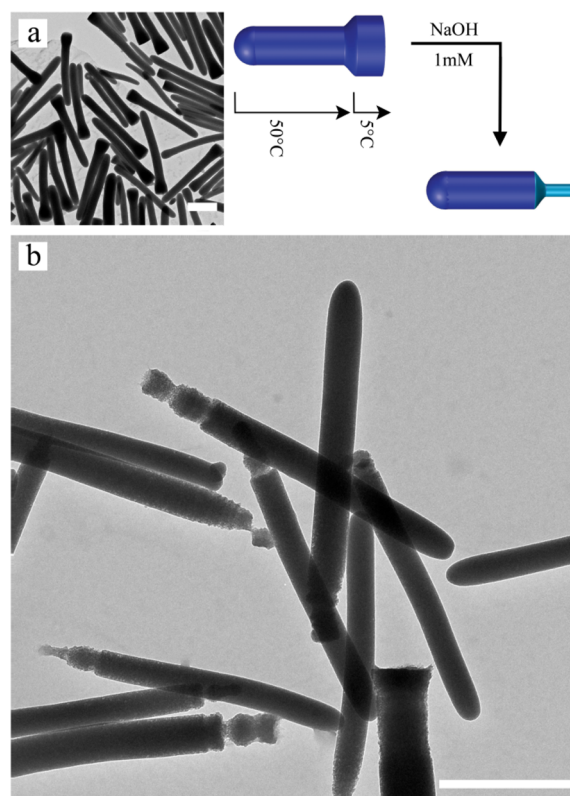


Figure 1. (a) Silica rods grown with a 50 °C (2 h) segment and a 5 °C (22 h) segment. (b) The same rods after etching in 1 mM of NaOH for 24 h. Scale bars indicate 1 μm .

the mild base. This is probably caused by the higher temperature during the growth of the first segment that makes this segment more resistant against etching.

By programming a sequence of temperatures during the growth of silica rods, we tuned the degree of silica condensation present in the particles and thus obtained a large variety of new particle morphologies after etching in a NaOH solution. In the following, we illustrate this general method with some specific examples: we prepared silica rods with a segment grown at 5 °C followed by a segment grown at 25 °C. Upon etching these particles in a 1 mM NaOH solution ([Figure 2a](#)), the tips of the particles preferentially etched, while at the boundary between the two segments the particles etched less. The remaining part of the rod etched as explained and shown in a previous paper in a cone shape.²⁷ As mentioned, the lower temperature during the first 2 h of the reaction lowered the degree of condensation of the silica network and caused an increase in the etching rate of the segment. Moreover, a thin silica shell surrounded the empty first segment grown at 5 °C. This thin shell was also observed in etching “regular” silica rods in 2 mM NaOH and was explained by the condensation of some of the silica precursor directly from the oil phase, but with a higher degree of siloxane cross-linking than the silica grown from the water droplet.²⁷ This shell becomes thinner when going from the rounded end to the flat end, because the exposure time to the growth solution decreases in this direction. The slight chemical gradient present in the bulk of the silica rods prepared using the general reaction procedure was not affected. Solely the part grown at lower temperatures was affected.

More complex shapes can be prepared by creating a more complicated sequence of growth steps with varying temper-

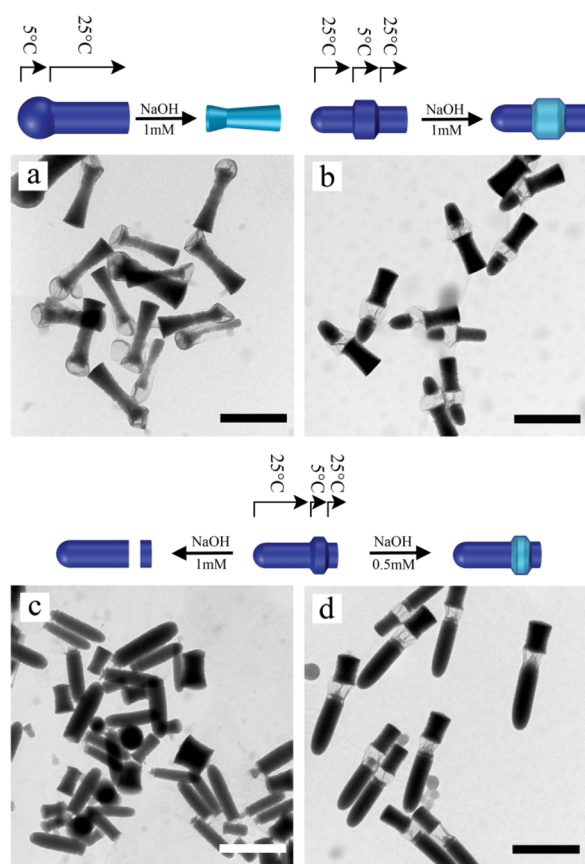


Figure 2. (a) Etched silica rods grown with a 5 °C (2 h) segment and a 25 °C (22 h) segment, etched at 1 mM of NaOH for 24 h. (b) Etched silica rods grown with a 50 °C (0.5 h), 5 °C (4 h), and 25 °C (22 h) segment, etched at 1 mM of NaOH for 24 h. (c) Etched silica rods grown with a 50 °C (1 h), 5 °C (4 h), and 25 °C (22 h) segment, where the first segment is grown slightly longer, etched at 1 mM of NaOH for 24 h. (d) Particles shown in part c but etched at 0.5 mM of NaOH for 24 h. Scale bars indicate 1 μm . Particles before etching are shown in Figure S11.

ature. For example, we prepared silica rods consisting of a thicker but less condensed middle segment. We achieved this by using three growth steps, where the first was grown at 25 °C, the second segment was grown at 5 °C, and the final segment was grown at 25 °C. Upon etching these silica rods in 1 mM NaOH the middle segment preferentially dissolved (Figure 2b), while keeping the dense outer shell in place, thus preventing the rod from breaking up. The first and last segments of the particle show a tendency to assume a cone-like shape, which is due to the gradient in composition along the length of the rod.

The hollow segment can be easily positioned at different positions along the length of the rod. By increasing the growth time of the first segment (25 °C), the second soluble segment (5 °C) shifts toward the flat end of the particle. Figure 2c shows etched particles grown with the soluble segment even closer to the flat end. We find that these particles break into two separate parts because the outer shell keeping the two segments together was completely etched away. This breakage could be prevented by etching these particles at a slightly lower concentration of base (0.5 mM NaOH), see Figure 2d. The length of this soluble segment can be easily changed: upon increasing the growth time the segment becomes larger and upon decreasing the growth time the segment becomes shorter.

An interesting phenomenon can be observed upon growing a third segment at increased temperature (50 °C). These particles now consist of a thin segment grown at 5 °C, a thick segment grown at 50 °C, and another thin segment grown at 50 °C. After etching these particles in 1 mM NaOH we find that the second segment has hardly dissolved (Figure 3

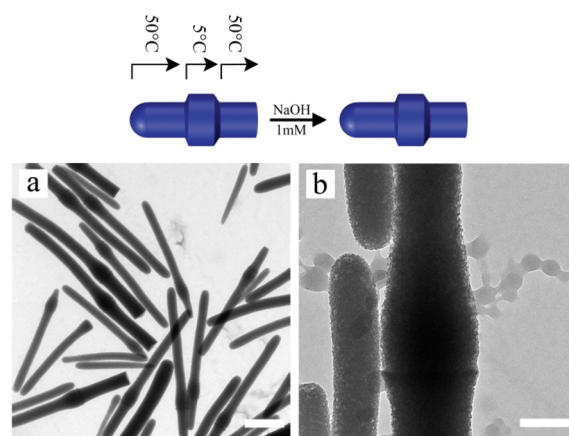


Figure 3. (a) Silica rods grown with a 50 °C (2 h), 5 °C (22 h), and 50 °C (18 h) segment, etched at 1 mM of NaOH. (b) The same particles at increased magnification. Scale bar indicates 1 μm (a) and 200 nm (b). Particles before etching are shown in Figure S11.

compared to Figure 1b). We attribute this to a continuing condensation during the final high 50 °C temperature step that strengthened the previously formed silica network enough to slow down dissolution. Between the second and third segments a step in contrast can be observed; here a small step in the silica microstructure was still present (Figure 3b).

In summary, the microstructure of the silica network is influenced by the growth conditions. The microstructure of the silica network influences the etching rate of the silica network, which at the macro level can be used to change the shape of the particle. Along with the temperature, it is expected that other growth parameters influence the particle structure during the growth.

Varying the Precursor (TEOS) Concentration. Other subtle changes in the growth conditions are expected to also give rise to changes in the silica network. In earlier work²⁷ we have shown that a gradual change in reaction conditions, due to the consumption of TEOS and the production of ethanol, resulted in a slight gradient in the degree of condensation of the silica present throughout the length of the particle. The main cause for this gradient was found to be the concentration of precursor, which decreased during the course of the reaction. To show the influence of the reactant concentration, here we changed the concentration of the precursor TEOS in steps. Upon injecting fresh, nonhydrolyzed TEOS 24 h after the start of the rod growth, we find that the particles continued growth, as described by Kuijk et al.²⁴ Only the length of the particles increased, and no step in diameter was observed in this case. The segment was allowed to continue growth for another 24 h, after which the particle increased in length to 1820 ± 196 nm, an increase by a factor 2. Upon etching these particles in 1 mM NaOH, the second segment etched into a cone shape, whereas the first segment appeared unaffected (Figure 4a). Clearly, a step in silica microstructure was introduced at the moment that the precursor was injected. The increased reaction rate as a result of a higher concentration of reactant apparently led to

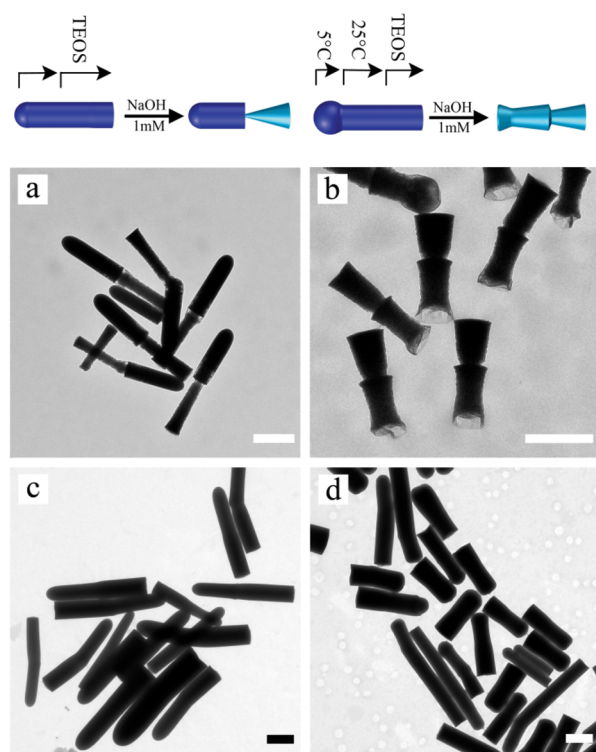


Figure 4. Silica rods grown with a second TEOS addition and etched in 1 mM NaOH for 24 h. Etched silica rods grown with a (a) 25 °C segment and continued growth at 25 °C (150 μ L of TEOS) and (b) 5 °C, 25 °C, and continued growth at 25 °C (100 μ L of TEOS). Scale bars indicate 1 μ m. Particles before etching are shown in parts c and d, respectively.

more quickly dissolving (i.e., less condensed) silica. Immediately after the addition of fresh reactant, the conditions were quite similar to those at the start of the reaction. However, as the reaction continued the concentration of available TEOS fell gradually and therefore this segment contained a gradient in the chemical microstructure. Also in the first segment the gradient in the microstructure should still be present. However, due to a continued deposition of TEOS from the oil phase, the shell around the first segment became thicker and protected this part against etching. Careful inspection of the particles in Figure 4a shows the first signs of etching in the last part of the first segment, supporting our hypothesis. This is caused by the thinner outer shell present around this part of the particle.

Sequential Steps. It is also possible to combine these methods and to create more complicated chemical composition sequences throughout and thus morphologies throughout the particle. As an illustration, we synthesized particles that were first grown at 5 °C for 4 h and then at 25 °C for 22 h, and finally after injection of fresh precursor the growth was continued for another 24 h at 25 °C. According to the previously shown results this should lead to particles that consist of a highly soluble first segment, a segment with a gradient in structure, a sudden decrease in the degree of condensation, and finally a segment with a gradient in structure. Indeed, upon etching these particles in 1 mM NaOH solution we find that the first segment dissolved preferentially to a hollow shell, while the second and third segments both etched into cone shapes (Figure 4b). Comparing the result to Figure 4a, we find that the second segment now also transformed into a cone shape; due to the decreased amount of TEOS used for

the extended growth of the silica rods, 100 μ L versus 150 μ L, the growth of the shell is less, making the inside of the particles more accessible to the etchant. Thus, we created a blunt cone with a second cone attached to its back. These results show that by changing the chemical composition in a smart way, the shape of the rod can be tuned by etching in low concentrations of NaOH.

Ethanol Delay Time. Datskos et al.²⁹ showed that the diameter of the rod is strongly influenced by the ethanol concentration. By delayed addition of ethanol, steps in the diameter could be achieved. Here, we show that changes in the ethanol concentration also influence the degree of silica cross-linking. First, a segment was grown for 3 h in the absence of ethanol. Then, the usual amount of ethanol was carefully mixed into the solution and the remaining part of the rod was left to grow for 24 h. Upon etching these particles in 1 mM NaOH, we found that the first segment, grown in the absence of ethanol, dissolved faster than silica grown under regular conditions (Figure 5a), again despite being thicker than the

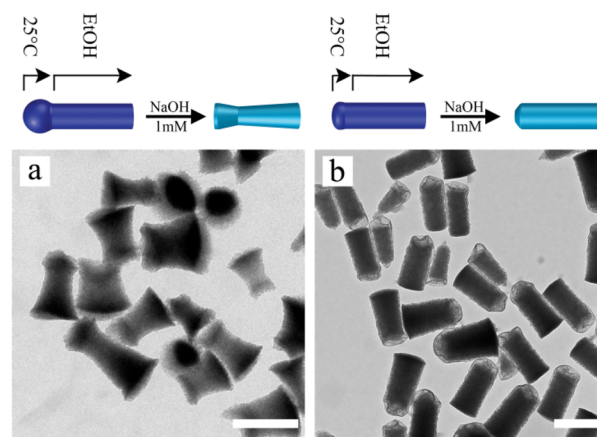


Figure 5. Silica rods etched at 1 mM NaOH for 24 h, prepared by growth of silica rods in the absence of ethanol for 3 h (a) and 1 h (b) and the continued growth in the presence of ethanol. Scale bars indicate 500 nm. Particles before etching are shown in Figure S12.

part of the rod that dissolved more slowly. The second segment etched into a cone, indicating that, after the delayed addition of ethanol, the gradient in structure, which can be found in regular silica rods, still formed. The length of this segment can be easily changed by choosing a shorter or longer time of growth without ethanol, as shown in Figure 5b. We propose the following mechanism: ethanol is a cosolvent in the reaction but is not consumed. Therefore, it does not have a direct influence on the reaction itself. However, ethanol partitions between the oil phase and the droplet phase. Datskos et al.²⁹ showed by dynamic light scattering that the volume of the droplet decreased upon the addition of ethanol to the reaction mixture.²⁹ The addition of ethanol increased the solubility of water in the pentanol phase. Due to this increase in solubility, the concentration of water inside the droplet decreases, leading to a lower formation rate of hydrolyzed TEOS. In turn, this resulted in a lower concentration of hydrolyzed TEOS inside the water droplet. As we have seen in the TEOS addition experiments this results in silica that dissolves more slowly.

Segmented Rods with Amine Functionality. Extending the above results to particles grown partly from silane coupling agents, which allow incorporation of functional groups inside hybrid organo-silica structures, we altered the chemical

properties of the rods by the co-condensation of the APTES (3-aminopropyltriethoxysilane), which was added 3 h after the start of the reaction. APTES has a structural formula similar to TEOS, but with one of the four ethoxy groups replaced by an aminopropoxy group. This group lowers the degree of condensation to a maximum of three bonds per silicon atom. Similarly as in the condensation of TEOS, however, a significant number of the silicon atoms ($\sim 30\%$) is not fully condensed and stays attached to hydroxy and/or ethoxy groups.^{15,16} Therefore, the incorporation of APTES is expected to increase the etching rate of the particle w.r.t. those composed of TEOS alone. For instance, working with silica core-shell-shell spheres, Chen et al.¹⁴ showed that the incorporation of a similar silane coupling agent (*N*-[3-(trimethoxysilyl)-propyl]-ethylene-diamine, TSD) in an inner shell in between a central TEOS based core and outer shell led to silica core-void-silica shell particles after etching with hydrofluoric acid through the outer silica shell. The Haes group incorporated APTES in a layer of organo-silica grown around metal core-shell particles and etched this layer through an outside Stöber silica layer using ammonia as the etchant.³² We adapted this concept to our silica rods. Adding APTES 3 h after the synthesis had begun resulted in particles with a normal silica segment and an APTES functionalized segment.

Upon etching undyed versions of these segmented particles in Milli-Q grade water, the second segment partly dissolved, whereas the first half remained intact as we expected (Figure 6a). Furthermore, the transition between the two parts appears to be rather sharp, and the location of the step in diameter can be easily tuned by choosing shorter or longer reaction times. Surprisingly, etching in basic conditions (3 mM NaOH) left the APTES segment intact and etched only the first segment, leaving behind a thin shell (Figure 6b). Contrary to what we expected and to what was observed by others,³² the APTES containing tail segment etched more slowly than the unmodified silica, which etched, as before, through an outer shell. At present we do not have an explanation for this behavior, which seems contrary to the etching results in water without base.

The presence of the APTES functionalized end segment on the rods could be illustrated by post-modification of the unetched particles from Figure 6 with a fluorescent dye that links to the amino group. The resulting dyed particles were imaged using a form of super-resolution microscopy, stimulated emission depletion (STED) confocal microscopy (see Figure 6c). Here, one can see that the functional amine groups can be found on both the tail of the particle and in a thin outer shell. The thin shell again originates from the attachment of the precursor directly from the oil phase and is similar to the layer found in earlier work.²⁷ The fluorescence from the shell is lower than that from the tail segment. The fluorescent segment appears to be shorter in length than the segment grown, but as described in earlier work, the dye cannot infiltrate the particle far enough. Nevertheless this confocal image gives a good indication that the functional group is distributed throughout the tail segment of the particles.²⁷ In the following we illustrate how differences in the rate of silica etching in both base and HF can be used to achieve unusual silica morphologies from spherical core-shell particles.

Silica Spheres—Different Etching Media. We also used spheres to illustrate the difference in etching rates between various etching media: HF, neutral, and basic NaOH etching. These spheres contained an internal layer of organo-silica

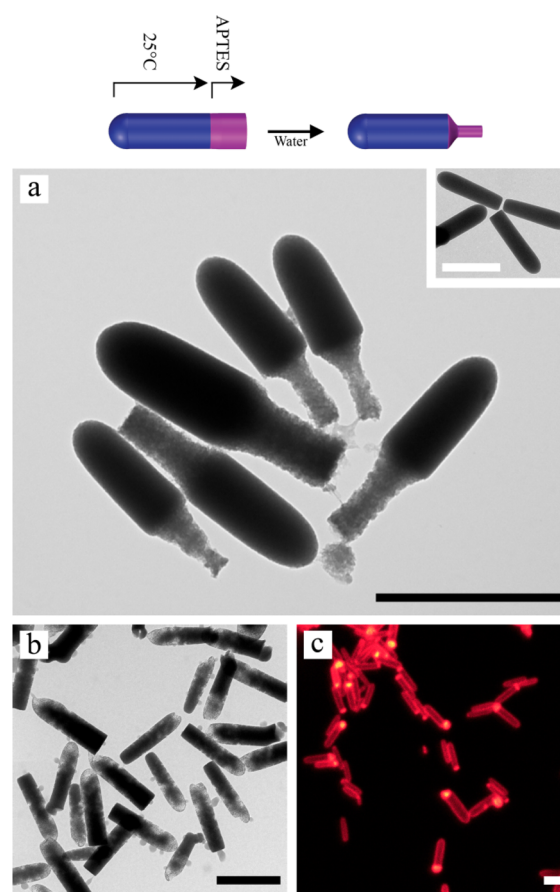


Figure 6. Silica rods with a step in composition. (a) Silica rods grown with an APTES segment etched for 24 h in Milli-Q grade water. (b) Silica rods grown with an APTES segment etched in 3 mM NaOH. (c) 2D-STED microscopy image of segmented fluorescent silica rods. Particles before etching are shown in the inset and Figure S13A. (Illustration) Blue: nonfunctionalized silica. Purple: APTES functionalized silica. Scale bars indicate 1 μm .

containing a silane coupling agent TSD (*N*-[3-(trimethoxysilyl)-propyl]ethylene-diamine) and a thin outer shell of pure silica, partially building upon Chen et al.¹⁴ (see schematic illustration in Figure 7). However, we used a higher concentration of TSD in the organo-silica segment. TSD is similar to APTES (used in the sections above), but its diamine arm is larger and contains an additional amine group.

Etching these particles with aqueous HF, the different etching rates of the organo-silica and pure silica became apparent. In the early stage of the etching process, the less condensed inner layer remained completely protected by the outer silica shell. However, as etching continued, the outer shell became progressively more porous and eventually the inner layer was exposed to the solution. Once the inner layer had become accessible, it was rapidly etched and removed (see Figure 7d) without the shells becoming more etched. When the inner layer was completely removed, a core-void-shell (or rattler) particle remained. We attribute the much higher dissolution rate of the inner organo-silica layer to its lower degree of condensation, similarly to the APTES segments in the silica rods described in the previous section.

The difference between the etching rates of the two types of silica depended strongly on the etchant. For HF etching, the difference was the largest. When the particles were etched in

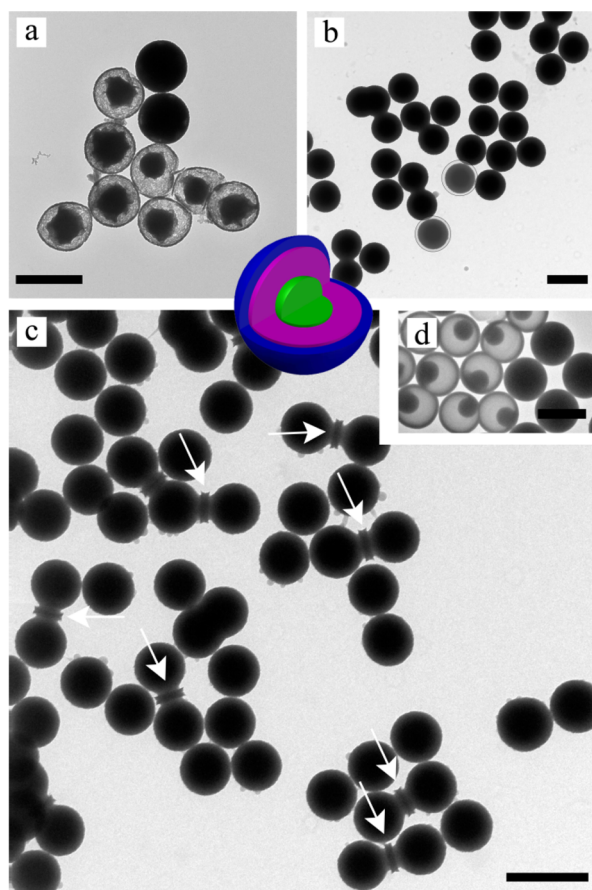


Figure 7. Core, inner layer, and outer shell silica spheres etched in (a) pure water; (b) mild basic conditions (1 mM NaOH, 24 h) where the original particle size is indicated for two particles with a gray circle, showing the difference in etching clearly compared to part a; (c) stronger basic conditions (4 mM NaOH, 24 h) showing silica dumbbells and triplet particles with ring shapes, with the part where the two single particles are connected (indicated by white arrows) being etched more slowly because it is more secluded and difficult to reach; and (d) 0.06% HF for 48 h. (Schematic Illustration) Green: fluorescent core. Purple: TSD functionalized layer. Blue: Pure silica shell. Scale bars indicate 1 μm .

pure water, the difference was smaller, although the inner layer still etched faster than the shell (see Figure 7a). When etching with NaOH, both types of silica etched at nearly identical rates. In 1 mM NaOH, the particles etched from the outside inward resulting in a uniform decrease in particle diameter, even beyond the thickness of the pure silica shell (see Figure 7b). The slight undercut of the inner layer under the silica shell, highlighted by the arrows in Figure 7c, indicates that the organo-silica etched slightly faster.

The silica etching rate was also affected by the geometric shape of the particle. This is clearly demonstrated by the etching behavior of dumbbell particles that were formed during the growth of the shell around the organo-silica layer ($\sim 23\%$). Upon etching these particles with 4 mM NaOH, the particles etched from the outside inward. However, a small segment of pure silica remained in the region between the two spherical lobes. This region is more secluded than the rest of the particle surface, and as a result it etched more slowly than the outer spherical parts. The dependence of the etching rates of different types of silica on etchant, geometry, and accessibility can be used to modify the shape of silica particles in new ways.

Silica Biconcave Platelets. The silica bridges visible for the dumbbell particles in Figure 7c are remnants of the silica shell and are sandwiched between two TSD functionalized layers. As described above, these layers etch much faster than pure silica in HF solution.¹⁴ By employing a second etching step using 0.03% HF, we specifically etched the organo-silica layer without significantly changing the shape of the bridge. This resulted in the release of biconcave platelets consisting of nonfunctionalized silica from the rest of the particle (Figure 8).

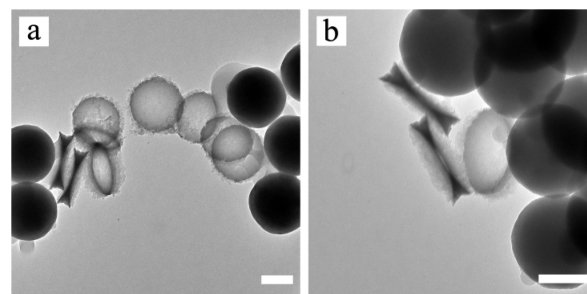


Figure 8. Silica biconcave platelets with an average diameter of 346 nm and an approximate thickness of 10 nm at the middle and 100 nm at the edge, prepared by first etching silica dumbbells in basic conditions and subsequently etching the particles with HF. Some of the detached core particles are also seen. Scale bar indicates 200 nm.

Some of these particles had an opening in the middle of the ring. This opening formed when the spheres had aggregated before the coating with the outer silica layer had commenced. In case there was no opening, the particles had aggregated after a thin silica layer had already grown between the two aggregated spheres. The biconcave platelets were monodisperse and had an average diameter of 346 ± 30 nm. The platelets had an approximate thickness of 10 nm in the middle and 100 nm at the edge and could in principle be separated from the other morphologies present by centrifugation.

CONCLUSIONS

In summary, we present a general method to change the chemical composition of rod-shaped and spherical core-shell silica particles. We found that a decrease in reaction temperature and an increase in precursor concentration result in a higher local rate of dissolution of the silica structure, when etched by NaOH solutions and vice versa. We found that an increase in the ethanol concentration during the reaction also resulted in an increased rate of dissolution of the grown segment. This allowed us to produce silica colloids in many new shapes: double cones, cylindrical rods, hollow middle segmented rods, rod-cone particles, and biconcave particles. A similar difference in dissolution rate could be induced by the incorporation of a silane coupling agent. Differences in local rates of dissolution were affected not only by the degree of condensation but also by other kinetic factors, such as the accessibility to the etchant used to create an even larger variety of particles. We used core-layer-shell silica spheres to illustrate the possibilities. These particles consisted of a core, an organo-silica layer, and a thin pure silica shell. Aggregates of these particles, formed during seeded growth, were found to etch anisotropically in NaOH solutions. The region close to the contact point between the spheres was found to etch more slowly due to its geometry. Using this finding, a silica platelet sandwiched between two silica spheres was obtained. More-

over, the resulting ring-like structures could be liberated from the organo-silica layer by a final HF etching resulting in biconcave ring shaped particles. We believe that these results open up new opportunities in the preparation and self-assembly of anisotropic particles.

■ EXPERIMENTAL SECTION

Silica Rods—General. Silica rods were synthesized as follows. First, 20.0 g of PVP (Sigma-Aldrich, $M_w = 40$ kg/mol) was dissolved in 200 mL of 1-pentanol (99%, reagent-plus, Sigma-Aldrich). After the PVP had completely dissolved 20.0 mL of ethanol (100%, Interchema), 5.6 mL of Milli-Q grade water (Millipore system) and 1.24 mL of 0.18 M sodium citrate solution in water (99%, Sigma-Aldrich) were added. After vigorous shaking of the flask, 4.5 mL of ammonia (26.3%, Sigma-Aldrich) was added. Before the addition of TEOS, the emulsion was split in volumes of 40.0 mL. To each volume 300 μ L of TEOS (tetraethyl orthosilicate, 98%, Sigma-Aldrich) was added, and the flask was shaken vigorously. If not mentioned otherwise, the particles were centrifuged after the reaction and redispersed in ethanol (100%, Interchema) and Milli-Q grade water (Millipore system) and again centrifuged and redispersed and stored in ethanol. The rods were used not older than one month.

Silica Rods—Temperature. In order to vary the chemical composition along the length of the rods, we changed the temperature during the course of the reaction. To this end we performed the reaction at a scale 40.0 mL of emulsion in a 40 mL vial. The vial was placed in a preheated hot air oven after the addition of TEOS. The bottles were cooled down at a slow rate to avoid strong convection in the bottle. The temperature was changed during the reaction in the following schemes:

- (1) 50 °C (2 h), 5 °C (22 h)
- (2) 50 °C (2 h), 5 °C (22 h), 50 °C (18 h)
- (3) 5 °C (2 h), 25 °C (22 h)
- (4) 50 °C (0.5 h), 5 °C (4 h), 25 °C (22 h)
- (5) 50 °C (1 h), 5 °C (4 h), 25 °C (22 h)

At the last step of reaction scheme 2, 70 μ L of TEOS (98%, Sigma-Aldrich) was also added to continue the growth of the rod and the reaction was left to continue for the above indicated time. A TEM (transmission electron microscopy) image of the nonetched silica rods is shown in the [Supporting Information](#) Figure S11.

Silica Rods—Precursor Concentration. The composition was also modulated by increasing the concentration of precursor. To this end, first a rod was grown for 24 h at room temperature as described above. Then 150 μ L of TEOS (98%, Sigma-Aldrich) was added, and the bottle was carefully homogenized. The synthesis was left undisturbed for another 24 h at room temperature. A TEM image of the nonetched silica rods is shown in [Figure 4c](#).

Silica Rods—Ethanol Addition Time. The addition moment of ethanol during the reaction was used to vary the degree of cross-linking of the silica rods. To this end, first a rod was grown following the general rod synthesis procedure, but in the absence of ethanol. The addition of ethanol was delayed by either 1 or 3 h. The reaction mixture was then left undisturbed for 24 h at room temperature. A TEM image of the nonetched silica rods is shown in the [Supporting Information](#) Figure S12.

Silica Rods—Sequential Steps. The above methods were combined by growing rods following the general rod synthesis procedure. The reaction temperature was kept at 5 °C for the first 4 h and subsequently raised to room temperature for another 22 h. Then 100 μ L of TEOS (98%, Sigma-Aldrich) was injected, and the mixture was carefully homogenized. The mixture was left to react for another 18 h. A TEM image of the nonetched silica rods is shown in the [Figure 4d](#).

Silica Rods with an APTES Segment. The procedure started with the general procedure described above. After mixing the content and the addition of TEOS, 40 mL of emulsion was transferred to a 40 mL glass bottle which was left to rest for 3 h. Then, 35.0 μ L of APTES (98%, Sigma-Aldrich) was added, and the mixture was carefully

homogenized and left to rest for 21 h. A TEM image of the nonetched silica rods is shown in the [Supporting Information](#) Figure S13A.

Organo-Silica Spheres. Silica spheres consisting of a fluorescently labeled silica core, an organo-silica layer, and a pure silica shell were synthesized as follows.

The preparation of the silica core consists of two phases. First the dye is coupled to the amine group on APTES. To this extent, 2 mL of absolute ethanol was added to 50.0 mg of FITC ($\geq 90\%$, HPLC grade, Sigma-Aldrich) and stirred for 15 min. Then, 300 μ L of APTES (98%, Sigma-Aldrich) was added, and the reaction mixture was stirred for 18 h in the dark. After coupling the dye to APTES, the fluorescently labeled core was prepared. In a round-bottom flask, 33.9 mL of ammonia (26.3%, Sigma-Aldrich) was mixed with 328 mL of absolute ethanol (Merck). To this mixture, 14.34 mL of TEOS (98%, Sigma-Aldrich) was added quickly while stirring vigorously. Finally, the mixture of FITC, APTES, and ethanol was added to the reaction mixture and left to react for 48 h.

A pure silica shell was grown around these particles to improve their stability. To 150.0 mL of unwashed reaction mixture two solutions (A and B) were added at a rate of 0.25 mL/h. The solution was stirred slowly during the whole reaction. Mixture A contained 1 mL of TEOS (98%, Sigma-Aldrich) and 6.9 mL of absolute ethanol (Merck) and mixture B contained 6.9 mL of absolute ethanol (Merck), 0.92 mL of ammonia (26.3%, Sigma-Aldrich), and 2.34 mL of Milli-Q grade water (Millipore system). Finally, the particles were washed three times with ethanol (100%, Interchema).

An organo-silica layer was grown around the fluorescent silica spheres as follows: 619 mL of absolute ethanol (Merck), 85.0 mL of Milli-Q grade water (Millipore system), 33.6 mL of ammonia (26.3%, Sigma-Aldrich), and 12.5 mL of seed particles (7.3 g/L) were added to a two necked round-bottom flask. Through one neck solution A was added, and through the second neck solution B was added. Solution A consisted of 32.3 mL of absolute ethanol (Merck), 10 mL of Milli-Q grade water (Millipore system), and 4.1 mL of ammonia (26.3%, Sigma-Aldrich). Solution B consisted of 31.3 mL of absolute ethanol (Merck), 11.8 mL of TEOS (98%, Sigma-Aldrich), and 3.82 mL of TSD (97%, Sigma-Aldrich). To prevent condensation at the nozzle of solution B, a slight nitrogen flow was applied away from the nozzle. Solution A was added to maintain a constant concentration of base.

Finally, a pure silica shell was grown using a regular Stöber silica growth procedure. To 140 mL of organo-silica coated cores (3.0 g/L), 913.5 mL of absolute ethanol (Merck), 121.5 mL of Milli-Q grade water (Millipore system), and 47.9 mL of ammonia (26.3%, Sigma-Aldrich) were added. While stirring, 8.98 mL of TEOS (98%, Sigma-Aldrich) was added in steps of 808 μ L every minute. Finally the particles were washed three times with ethanol (100%, Interchema). A TEM image of the nonetched silica rods is shown in the [Supporting Information](#) Figure S13B.

Etching. Silica rods were etched by dispersing 6 mg of preformed silica rods in 10 mL of NaOH (sodium hydroxide, Sigma-Aldrich, extra pure, pellets) solution and put on a roller bank for 24 h. The concentration of the base was varied at the mM level to change the degree of etching (see the [Results and Discussion](#) section).

Silica rods with an APTES segment were etched by transferring 6 mL of 1.4 g·L⁻¹ silica rods in ethanol to 40 mL of Milli-Q grade water (Millipore system). The bottle was put on a roller bank for 27 h. Next, the particles were washed three times with ethanol (100%, Interchema).

Silica spheres were etched in mild base by dispersing 6 mg of particles to 10.0 mL of 4 mM NaOH (sodium hydroxide, Sigma-Aldrich, pellets) solution and put on a roller bank for 24 h. Afterward the particles were washed three times with ethanol (100%, Interchema). To obtain biconcave disks, the particles were further etched in a solution of HF. To this end, 2.0 mg of etched silica spheres were dispersed in 10 mL of Milli-Q grade water (Millipore system). To this solution, 6.0 μ L of HF (40–45%, technical grade, Riedel-de Haën) was added and subsequently homogenized. The solution was immediately washed with ethanol three times. This last step was done quickly to stop the reaction immediately.

The particles were transferred from ethanol to the etching solution as follows. The samples were centrifuged, and the supernatant was decanted and redispersed in the etching solution. Traces of ethanol were minimized by drying the samples at room temperature using a flow of nitrogen. The particles are in a dry state for maximum 2 min. The concentration of the particles in the dispersion was measured by drying a small part of the dispersion and weighing the dry content.

Particle Characterization. Transmission electron microscopy images were obtained using a Philips Tecnai 12 electron microscope. The width and length of the particles were determined by measuring between 100 and 150 particles by hand using the TEM imaging platform iTEM. The width and length of the particles is given as follows: length or width \pm polydispersity. The polydispersity represents the standard deviation of the size distribution. CW-gated 2D STED confocal microscopy images of segmented silica rods were taken using a Leica TCS SP8 equipped with a continuous wave depletion laser. To resolve the fluorescence pattern of the particles, STED measurements were performed using a solid state laser at a wavelength of 592 nm. The particles were imaged in CW-STED mode by exciting fluorescein at 488 nm using a white light continuum laser. The images were taken at a resolution of 512×512 pixels (pixel size: $10.4 \text{ nm} \times 10.4 \text{ nm}$).

■ ASSOCIATED CONTENT

Supporting Information

The Supporting Information is available free of charge on the ACS Publications website at DOI: [10.1021/acs.chemmater.7b00687](https://doi.org/10.1021/acs.chemmater.7b00687).

TEM images of the silica rods prior to etching with NaOH ([PDF](#))

■ AUTHOR INFORMATION

Corresponding Authors

*(F.H.) E-mail: f.hagemans@uu.nl.

*(A.v.B.) E-mail: a.vanblaaderen@uu.nl.

*(A.I.) E-mail: a.imhof@uu.nl.

ORCID

Fabian Hagemans: [0000-0002-4748-8547](https://orcid.org/0000-0002-4748-8547)

Arnout Imhof: [0000-0002-7445-1360](https://orcid.org/0000-0002-7445-1360)

Author Contributions

The manuscript was written through contributions of all authors. F.H. wrote the manuscript and performed the synthesis and analysis of rod-shaped particles. F.H. performed the etching of the rod-shaped particles. W.V. and C.R. performed the synthesis of the spherical particles. W.V., C.R., and F.H. performed the etching of the spherical particles. A.v.B. and A.I. supervised the research. All authors have given approval to the final version of the manuscript.

Funding

This research is funded by The Netherlands Organisation for Scientific Research (NWO). A.v.B. acknowledges the European Research Council under the European Union's Seventh Framework Programme (FP/2007-2013)/ERC Grant Agreement No. [291667]. This work is part of the research program of the Foundation for Fundamental Research on Matter (FOM), which is part of The Netherlands Organisation for Scientific Research (NWO).

Notes

The authors declare no competing financial interest.

■ ACKNOWLEDGMENTS

The authors acknowledge Ernest van der Wee for performing the CW-gated 2D STED confocal microscopy measurements,

Albert Grau Carbonell for designing the 3D illustrations, and Douglas R. Hayden for careful reading of the manuscript.

■ ABBREVIATIONS

APTES, 3-aminopropyltriethoxysilane; PVP, polyvinylpyrrolidone; STED, stimulated emission depletion; TEM, transmission electron microscopy; TEOS, tetraethyl orthosilicate; TSD, *N*-[3-(trimethoxysilyl)propyl]ethylene-diamine

■ REFERENCES

- (1) Glotzer, S. C.; Solomon, M. J. Anisotropy of building blocks and their assembly into complex structures. *Nat. Mater.* **2007**, *6*, 557–562.
- (2) Yang, S.-M.; Kim, S.-H.; Lim, J.-M.; Yi, G.-R. Synthesis and assembly of structured colloidal particles. *J. Mater. Chem.* **2008**, *18*, 2177–2190.
- (3) Perro, A.; Reculosa, S.; Ravaine, S.; Bourgeat-Lami, E.; Duguet, E. Design and synthesis of Janus micro- and nanoparticles. *J. Mater. Chem.* **2005**, *15*, 3745–3760.
- (4) Rossi, L.; Sacanna, S.; Irvine, W. T. M.; Chaikin, P. M.; Pine, D. J.; Philipse, A. P. Cubic crystals from cubic colloids. *Soft Matter* **2011**, *7*, 4139–4142.
- (5) Sacanna, S.; Korpics, M.; Rodriguez, K.; Colón-Meléndez, L.; Kim, S.-H.; Pine, D. J.; Yi, G.-R. Shaping colloids for self-assembly. *Nat. Commun.* **2013**, *4*, 1688.
- (6) Nagao, D.; van Kats, C. M.; Hayasaka, K.; Sugimoto, M.; Konno, M.; Imhof, A.; van Blaaderen, A. Synthesis of hollow asymmetrical silica dumbbells with a movable inner core. *Langmuir* **2010**, *26*, 5208–5212.
- (7) Long, R.; Zhou, S.; Wiley, B. J.; Xiong, Y. Oxidative etching for controlled synthesis of metal nanocrystals: Atomic addition and subtraction. *Chem. Soc. Rev.* **2014**, *43*, 6288–6310.
- (8) Xie, F.; Ye, W.; Sun, H.; Kou, S.; Guo, X. Silver ions induce lateral etching of gold nanorods by K_2PtCl_4 . *Langmuir* **2015**, *31*, 6823–6828.
- (9) Deng, T.-S.; van der Hoeven, J. E. S.; Yalcin, A. O.; Zandbergen, H. W.; van Huis, M. A.; van Blaaderen, A. Oxidative etching and metal overgrowth of gold nanorods within mesoporous silica shells. *Chem. Mater.* **2015**, *27*, 7196–7203.
- (10) Brinker, C. J. Hydrolysis and condensation of silicates: Effects on structure. *J. Non-Cryst. Solids* **1988**, *100*, 31–50.
- (11) Iler, R. K. *The Chemistry of Silica: Solubility, Polymerization, Colloid and Surface Properties and Biochemistry of Silica*; Wiley: 1979; pp 896.
- (12) van Blaaderen, A.; Kentgens, A. P. M. Particle morphology and chemical microstructure of colloidal silica spheres made from alkoxysilanes. *J. Non-Cryst. Solids* **1992**, *149*, 161–178.
- (13) Bergna, H. E., Ed. *The Colloid Chemistry of Silica*; Advances in Chemistry Series; American Chemical Society: 1994; Vol. 234.
- (14) Chen, D.; Li, L.; Tang, F.; Qi, S. Facile and scalable synthesis of tailored silica 'nanorattle' structures. *Adv. Mater.* **2009**, *21*, 3804–3807.
- (15) van Blaaderen, A.; Vrij, A. Synthesis and characterization of colloidal dispersions of fluorescent, monodisperse silica spheres. *Langmuir* **1992**, *8*, 2921–2931.
- (16) van Blaaderen, A.; Vrij, A. Synthesis and characterization of monodisperse colloidal organo-silica spheres. *J. Colloid Interface Sci.* **1993**, *156*, 1–18.
- (17) Wong, Y. J.; Zhu, L.; Teo, W. S.; Tan, Y. W.; Yang, Y.; Wang, C.; Chen, H. Revisiting the Stöber method: Inhomogeneity in silica shells. *J. Am. Chem. Soc.* **2011**, *133*, 11422–11425.
- (18) Bazula, P. A.; Arnal, P. M.; Galeano, C.; Zibrowius, B.; Schmidt, W.; Schüth, F. Highly microporous monodisperse silica spheres synthesized by the Stöber process. *Microporous Mesoporous Mater.* **2014**, *200*, 317–325.
- (19) Li, S.; Wan, Q.; Qin, Z.; Fu, Y.; Gu, Y. Understanding Stöber silica's pore characteristics measured by gas adsorption. *Langmuir* **2015**, *31*, 824–832.
- (20) Tan, L.; Liu, T.; Li, L.; Liu, H.; Wu, X.; Gao, F.; He, X.; Meng, X.; Chen, D.; Tang, F. Uniform double-shelled silica hollow spheres:

Acid/base selective-etching synthesis and their drug delivery application. *RSC Adv.* **2013**, *3*, 5649–5655.

(21) Zhang, Q.; Ge, J.; Goebel, J.; Hu, Y.; Lu, Z.; Yin, Y. Rattle-type silica colloidal particles prepared by a surface-protected etching process. *Nano Res.* **2009**, *2*, 583–591.

(22) Hu, Y.; Zhang, Q.; Goebel, J.; Zhang, T.; Yin, Y. Control over the permeation of silica nanoshells by surface-protected etching with water. *Phys. Chem. Chem. Phys.* **2010**, *12*, 11836–11842.

(23) Liu, B.; Zhang, C.; Liu, J.; Qu, X.; Yang, Z. Janus non-spherical colloids by asymmetric wet-etching. *Chem. Commun.* **2009**, 3871–3873.

(24) Kuijk, A.; van Blaaderen, A.; Imhof, A. Synthesis of monodisperse, rodlike silica colloids with tunable aspect ratio. *J. Am. Chem. Soc.* **2011**, *133*, 2346–2349.

(25) Zhang, J.; Liu, H.; Wang, Z.; Ming, N. Au-induced polyvinylpyrrolidone aggregates with bound water for the highly shape-selective synthesis of silica nanostructure. *Chem. - Eur. J.* **2008**, *14*, 4374–4380.

(26) Kuijk, A.; Imhof, A.; Verkuijlen, M. H. W.; Besseling, T. H.; van Eck, E. R. H.; van Blaaderen, A. Colloidal silica rods: Material properties and fluorescent labeling. *Part. Part. Syst. Charact.* **2014**, *31*, 706–713.

(27) Hagemans, F.; van der Wee, E. B.; van Blaaderen, A.; Imhof, A. Synthesis of cone-shaped colloids from rod-like silica colloids with a gradient in etching rate. *Langmuir* **2016**, *32*, 3970–3976.

(28) Datskos, P.; Sharma, J. Synthesis of segmented silica rods by regulation of the growth temperature. *Angew. Chem., Int. Ed.* **2014**, *53*, 451–454.

(29) Datskos, P.; Chen, J.; Sharma, J. Addressable morphology control of silica structures by manipulating the reagent addition time. *RSC Adv.* **2014**, *4*, 2291–2294.

(30) Zhang, A.-Q.; Li, H.-J.; Qian, D.-J.; Chen, M. Kinetically-controlled template-free synthesis of hollow silica micro-/nanostructures with unusual morphologies. *Nanotechnology* **2014**, *25*, 135608.

(31) Brinker, C. J.; Sehgal, R.; Hietala, S. L.; Deshpande, R.; Smith, D. M.; Loy, D.; Ashley, C. S. Sol-gel strategies for controlled porosity inorganic materials. *J. Membr. Sci.* **1994**, *94*, 85–102.

(32) Roca, M.; Haes, A. J. Silica-void-gold nanoparticles: Temporally stable surface-enhanced raman scattering substrates. *J. Am. Chem. Soc.* **2008**, *130*, 14273–14279.